The Impact of Polypropylene-*graft*-Maleic Anhydride on the Crystallization and Dynamic Mechanical Properties of Isotactic Polypropylene

David P. Harper,[1] Marie-Pierre G. Laborie,[2] Michael P. Wolcott[2]

[1]*Tennessee Forest Products Center, University of Tennessee, Knoxville, Tennessee 37996*
[2]*Department of Civil and Environmental Engineering, Washington State University, Pullman, Washington 99164*

Received 11 March 2008; accepted 21 July 2008
DOI 10.1002/app.29100
Published online 13 October 2008 in Wiley InterScience (www.interscience.wiley.com).

ABSTRACT: Differential scanning calorimetry (DSC) and dynamic mechanical analysis (DMA) were used to identify the mechanisms that lead to differences in the mechanical behavior of formulations of polypropylene blended with maleated polypropylene (MAPP) copolymers. MAPP lowered the melting temperature of PP indicating that less stable crystals were formed possibly because of cocrystallization of PP and MAPP. Crystallization kinetics revealed that copolymers do not change the rate of crystal growth, but may retard nucleation leading to a more spherulitic morphology. The dynamic storage modulus slightly increased in the glassy region with the small addition amounts of MAPP, while mechanical dampening systematically decreased with MAPP addition. An analysis of the viscoelastic behavior did not reveal any real differences in molecular coupling around the β-transition of PP with the addition of the MAPP copolymer. At low addition levels, MAPP does not appear to have a significant impact on the viscoelastic properties of the polymer blend. © 2008 Wiley Periodicals, Inc. J Appl Polym Sci 111: 753–758, 2009

Key words: polypropylene; viscoelastic properties; crystallization; cooperative effects; copolymer

INTRODUCTION

The addition of functionalized copolymer-coupling agents such as polypropylene-*graft*-maleic anhydride (MAPP) is often used in melt-blended composites and blends to enhance the adhesive interaction with fibers and other polymer phases. For instance, a 2% MAPP addition to a Wood-PP composite improves bending strength by 50% and stiffness by 27%.[1] Previous research has indicated that formulations with MAPP alone or in the presence of a reinforcing fiber may alter the crystal morphology of PP.[2] However, the size of the grafted MA groups is such that they do not participate in chain folding.[3] The reactive sites always exist in the amorphous regions. This has the potential to hindering the molecular mobility of adjacent molecules. In fact, we hypothesize that molecular interactions between PP and MAPP coupling agent likely increase intermolecular coupling. However, simultaneously, the presence of the MA will have a negative impact on the crystalline structure of the polymer.

The mechanism by which MAPP impacts bulk performance of a composite is not wholly understood. A study of intermolecular interactions and morphology in blends of MAPP and PP is needed to elucidate the coupling mechanism in WPC formulations. Such a study will help link blend properties and performance to the molecular and supramolecular organization of the homopolymer. This study aims at characterizing morphological and mechanical properties of PP/MAPP blends commonly used in composite extrudates. Specific goals are to evaluate the impact of MAPP on the crystallization, molecular interaction, and viscoelastic properties of PP and then to relate morphology to mechanical performance.

Such morphological information can be obtained with thermal analysis methods. Namely, the comparison in glass and melt transitions in blends with respect to the pure polymers reveals the morphology of the amorphous and crystalline phases, respectively. In miscible amorphous polymer blends, one glass transition intermediate of that of the pure polymers is observed. Miscibility also causes an asymmetric broadening of the glass transition dispersion toward low frequencies.[4] Recent models describing

Correspondence to: D. P. Harper (dharper4@utk.edu).
Contract grant sponsor: Office of Naval Research; contract grant number: N00014-00-C-0488.

the temperature dependence of segmental relaxation in amorphous polymers can be used to assess the strength of intermolecular interactions. Such models, first introduced by Angell and coworkers, use the concept of fragility.[5] Fragile glass formers exhibit strong intermolecular interactions and are associated with a broad distribution of relaxation times and non-Arrhenius behavior. Strong glass formers on the other hand display weak intermolecular interactions, near monoexponential segmental relaxation and near Arrhenius temperature dependence of the characteristic relaxation time (τ). Fragility (m) can then be determined from the slope of an Arrhenius plot normalized to T_g, also called fragility plot[5]:

$$m = \left. \frac{d \log\langle\tau\rangle}{d\left(T^* \Big/ T\right)} \right|_{T=T^*} . \quad (1)$$

In eq. (1), τ is the characteristic relaxation time, T is the temperature at τ, and T^* is the reference temperature. High values of m indicate a fragile glass. For miscible polymer blends, the constraints on molecular motion increase when the number of couplings within the same chain is increased.[6] That is to say, as molecular interactions increase so does fragility. This fragility increase has been observed in miscible blends with large ΔT_g and strong hydrogen bonding.[7,8]

Although fragility studies are valuable to characterize blend interactions in the amorphous phase, crystallization kinetics and degree of crystallinity can also shed light on miscibility in the molten and crystalline phases. For blends that are miscible in the liquid phase, a melting point depression is observed. Melting point depression is based upon the assumption that the entropic contribution to mixing is negligible. Although this is a reasonable assumption for high-molecular weight polymers,[9] the blends considered in this study comprise low-molecular weight additives and may not abide to this assumption.

A depression in the crystallization temperature (T_c) is also observed for blends that are miscible in the molten state. In fact, in miscible polymer blends, specific intermolecular interactions are likely to inhibit the chain mobility and compete with phase separation during crystallization.[10] As a result, crystallization rate and especially spherulitic growth rate may be reduced.[11] Both phenomenona, crystallization and nucleation mechanisms can be described with Avrami model[12] and/or the Lauritzen–Hoffman model.[13] According to Avrami kinetics, the change in degree of crystallinity $\chi(t)$ with time (t) during isothermal crystallization can be described by:

$$\ln[-\ln(-\chi(t))] = \ln k + n \ln[t], \quad (2)$$

where $\chi(t)$ ranges from 0 to 1, n is the Avrami exponent, and k is the crystallization rate constant. The Avrami exponent is dependent on both the nucleation mechanism and density. This dependence leads to a relationship between n and crystal shape. Differential scanning calorimetry (DSC) is ideally suited to determine the Avrami constants because the heat evolved during an isothermal crystallization scan as a function of time, $H(t)$, can be converted into a relative degree of crystallinity.

$$\chi(t) = \frac{\int_0^t (dH/dt)dt}{\int_0^\infty (dH/dt)dt}. \quad (3)$$

Practically, the Avrami model is valid for low degrees of crystallinity ($\chi(t) < 0.5$). At higher degrees of crystallinity, other mechanisms control crystallization, such as crystallite impingement and chain diffusion. Another limitation of the Avrami model is that an overall rate of crystallization rather than a rate of nucleation and lamellar growth rate are measured. Yet, these mechanisms occur at specific, independent rates. These rates can be calculated with the Lauritzen–Hoffman growth rate theory:

$$\ln G = \ln G_0 - \frac{U^*}{R(T_c - T_\infty)} - \frac{K_g}{T_C \Delta T f}, \quad (4)$$

Where G is the linear lamellar growth rate, G_0 a constant preexponential factor, U^* the activation energy for chain reptation, K_g the nucleation constant that relates to the lamellar surface energetics, and T_c the crystallization temperature.[13] The degree of supercooling, ΔT, is the difference between the isothermal crystallization temperature and the equilibrium melting point T_m°; T_∞ is the temperature at which all flow and reptation ceases (estimated at $T = 232$ K)[14] and R the ideal gas constant. T_m° can be determined from the intercept of the experimental data T_m versus T_c and the equation $T_m^\circ = T_c^\circ$, although the nonlinearity of the relationship and the need for extrapolation can lead to large errors in estimates T_m°.[15,16] Assuming athermal nucleation ($n = 3$) and spherulitic crystallite shapes, Avrami kinetics can be related to Lauritzen–Hoffman secondary nucleation theory[13]:

$$k = \frac{4}{3}\pi G^3 N. \quad (5)$$

where N is the number of nuclei. This simplification is adequate when there is no homogeneous nucleation present and for low χ before impingement occurs. Therefore, a relationship exists between the time at a specified degree of crystallization (t_χ) (e.g., $\chi = 0.5$) and G:

$$t_\chi^{-1} = A_1 G_0 \exp\left(-\frac{U^*}{R(T_C - T_\infty)} - \frac{K_g}{T_C(\Delta T)f}\right). \quad (6)$$

Where A_1 is an arbitrary proportionality constant.

The crystallization kinetics indicates how MAPP is impacting the development of PP crystal morphology. The inclusion of grafted sites on the PP backbone may impede the crystallization process and slow the crystal growth process.

MATERIALS AND METHODS

Sample preparation

Isotactic polypropylene (PP) (Solvay HB 9200, M_n = 35,000 g/mol) and maleic anhydride polypropylene (MAPP) (Honeywell A-C 950P, M_n = 8000 g/mol, SAP = 45 KOH/g) were obtained from Honeywell. Specific formulations known to impart different properties to the final composite were prepared for DSC and dynamic mechanical analysis (DMA).[17] Sixty grams of each blend was first compounded in a Thermo Haake mixing head at 180°C at 120 rpm with Braburn rollers for 8 min. The blends were then placed in a capillary rheometer (Rheometrics Acer) with a barrel temperature of 180°C. The blends had a dwell time of 10 min in the barrel before being transferred to a mold for DMA specimens, 1.6 mm × 6 mm × 45 mm. The mold temperature was 110°C and the specimens were removed quickly after molding. DSC specimens were obtained by grinding the molded blends to a 60 mesh with a laboratory Wiley mill. The formulations selected for DSC and DMA analyses consisted of PP/MAPP blends with varying weight ratios: 100 : 0, 99 : 1, 98 : 2, 95 : 5, 85 : 15; neat MAPP was also evaluated by DSC for comparison.

Thermal analysis

Approximately 7 mg of powder compound was placed in 40-μL hermetically sealed pans and submitted to DSC for crystallization and glass transition temperature behaviors. The DSC temperature program consisted of (1) ramp from 25 to 200°C at 20°C/min, (2) soak for 10 min, (3) cool at 20°C/min to a selected crystallization temperature, T_c, (4) hold at T_c until crystallization is complete, (5) cool from T_c to −20°C at 20°C/min, (6) ramp from −20 to 10°C at 10°C/min to capture the glass transition, and finally (7) heat from 10 to 200°C at 20°C/min to capture the melting temperature. The glass transition (T_g) was defined as the midpoint in the change of baselines obtained on segment 6, and the melt temperature was defined by the end of the melt endotherm at the intersection between the baseline and the trailing slope on segment 7.

DMA specimens, 1.6 mm × 6 mm × 45 mm, were tested in a Rheometrics RSA II solids analyzer in dual cantilever mode. The strain level for linear viscoelasticity was first determined at 0.1% by performing static strain sweeps at extreme temperatures −50, 25, and 100°C. With this strain level, the samples were submitted to a step-frequency sweep from −50 to 100°C using 2°C increments with a 1-min soak time and dynamic loading from 1 to 10 Hz with three replicates.

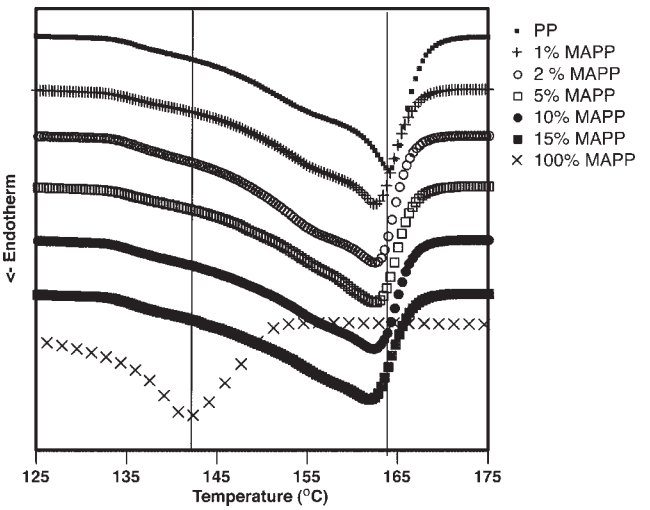

Figure 1 DSC melt curves for binary blends of PP MAPP isothermally crystallized at 130°C.

RESULTS AND DISCUSSION

Melt behavior

The DSC traces for neat PP reveals two melting points with a peak temperature around 159 and 165°C (Fig. 1). A double melting endotherm for isotactic PP is consistent with the existence of two crystal forms with distinct lamellar thickness and thermal stability.[18–22] Neat MAPP melts at 142°C, ~ 20°C below PP. In the MAPP/PP blends, only one melting point around 165°C, characteristic of PP, remains. This melting point presents two shoulders reminiscent of the two individual melting points of neat PP, which appear to have merged into a broad endotherm in the blends. Integration of the endotherm reveals that neat PP and the blends have a similar degree of crystallinity, around 65% ± 2% when considering a perfect crystal to have an enthalpy of melting of 165 J/g.[23] In the blends, the higher melt temperature of PP is depressed to varying degrees by the presence of MAPP (Fig. 1). The depression of PP melting point with increasing MAPP content suggests the occurrence of cocrystallization and/or defect insertion or isomorphic crystallization of MAPP and PP in the blends. The absence of a distinct MAPP melting point in the blends indicates that pure MAPP crystalline structures are not detected, maybe because of their small proportion in the blend or due to the fact that they cocrystallize with PP. The hypothesis of cocrystallization of

TABLE I
Kinetic Parameters Obtained from the Avrami Analysis (n) and the Lauritzen–Hoffman (K_g) for Neat PP and the Binary Blend of PP and 5% MAPP

	$n \pm 0.04$	K_g (K^2) $\pm$ 0.6
PP	2.71	−20.6
95% PP/5% MAPP	2.91	−21.0
P-value	0.003	0.292

The *P*-value in each column indicates the results for the *t*-test ($\alpha = 0.05$).

MAPP and PP is consistent with previous studies, which have shown the existence of MAPP within the spherulitic structure of PP[1,24] and the formation of isomorphic crystals in MAPP/PP blends.[25]

Kinetic results

To further determine the blends morphology and crystallization kinetics, Avrami and Lauritzen–Hoffman analyses were conducted on the neat PP and the 95 : 5 PP/MAPP blend. The Avrami exponent (n) characterizes the crystal morphology,[23] whereas the Lauritzen–Hoffman kinetics allows characterizing the lamellar surface free energy using the parameter K_g, where K_g scales with the product of the lateral surface free energy (σ_l) and the fold surface energy (σ). The results of the two analyses on neat PP and on the 95 : 5 PP/MAPP blend are summarized in Table I along with the result of a *t*-test ($\alpha = 0.05$) to detect statistical differences in the kinetic parameters. Table I shows that with the addition of 5% MAPP, the Avrami coefficient increases slightly but significantly from 2.71 to 2.91. This indicates a change from a truncated shape to a purely spherelitic shape as indicated by $n = 3$. The growth kinetics of the polymer was further examined using Lauritzen–Hoffman secondary nucleation theory with the required assumption of $n = 3$. No significant difference in the K_g values of the blends is observed (Table I). This indicates that the energetics of nucleation is similar in neat PP and in the 95 : 5 PP/MAPP blend. This observation is consistent with previous results indicating no change in growth rates for similar levels of MAPP.[2]

Dynamic mechanical response

Pure PP displays two transitions in the −50 to 100°C temperature window as demonstrated by a drop in storage modulus and a damping peak (Fig. 2). The temperature transition around 0°C is the β-relaxation and it is associated with the glass-rubber transition of the fully amorphous phase.[26] The temperature transition between 40 and 60°C is the α-relaxation or glass-rubber transition of the bound, constrained amorphous phase surrounding the crystals.[26] The MAPP has no apparent impact on the location of the β-transition (Table II). At low MAPP addition levels, the PP/MAPP blends display a slightly higher E' in the glassy region than pure PP with the exception of the 15% MAPP loading where E' is decreased (Fig. 2). The slightly reduced modulus at 15% addition MAPP level may be speculated as the result of small changes in crystal structure or phase separation resulting from a high MAPP loading, but neither was evidenced in this study. Nevertheless, the modulus in the rubbery region is similar for all blends, which arises from the combination of properties from each polymer. The addition of MAPP decreases

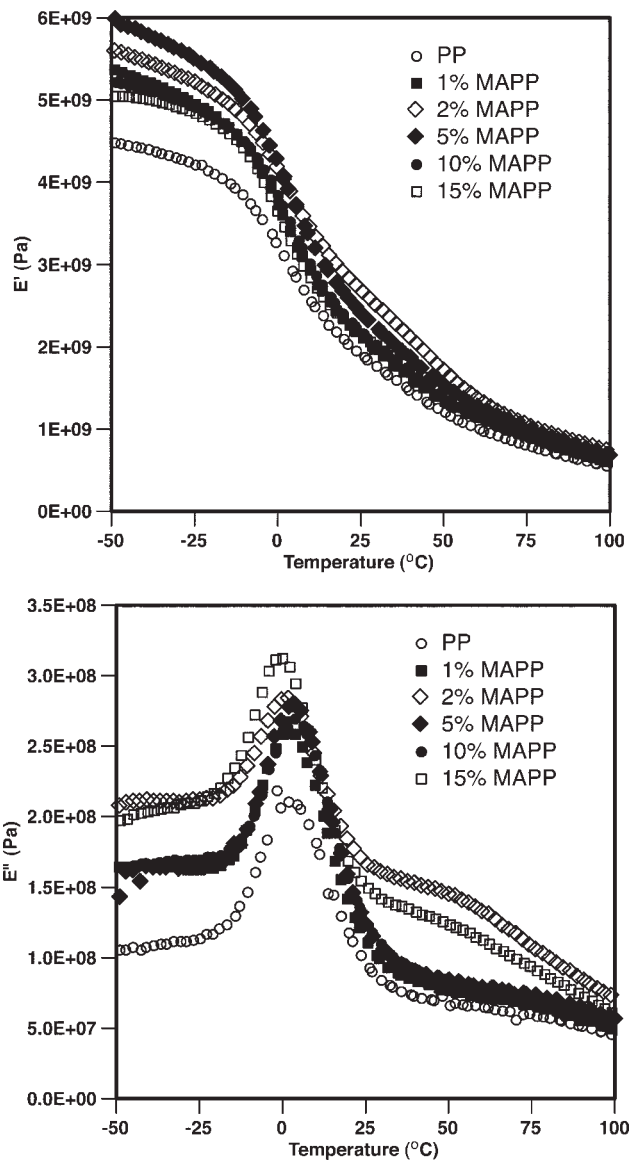

Figure 2 DMA temperature scans of binary polymer blends of PP and MAPP showing storage modulus (E') (top) and loss modulus (E'') (bottom). (The traces were obtained at 1 Hz using a 2°C steps and soaking for 1 min at each temperature).

TABLE II
The β Transitions (°C) of PP Obtained for Different Blends Determined by DMA and the Peak in E'' for an Average of Three Specimens at 1 Hz

Weight % additive	PP/MAPP
0	−0.3
1	−0.5
2	−1.5
5	1.7
10	−2.6
15	−2.2

The values are an average of three runs with an estimated error of ±1.0°C.

the magnitude of E'' over the whole temperature range investigated, which could be caused in part by the more restricted mobility or to the lower damping of the polar MAPP copolymer compared with PP. This observation is consistent with results on wood plastic composites, where MAPP has also been shown to decrease damping.[27]

When considering blends of semicrystalline polymers, one may expect to find the broadening of the β-transition with increased interaction between miscible polymers in the amorphous phase. A degree of cooperative chain movement in the amorphous fraction has shown agreement between amorphous PP and isotactic PP when a normalized Arrhenius equation was used.[28] Thus, from the principle of time-temperature superposition (TTSP), the shift factor (a_T) may be used to determine the fragility factor, m, provided that thermorheological simplicity and linear viscoelasticity are obeyed.

TTSP was performed on E' and E'' for all blends by using horizontal shifts referenced to the peak in E'' (Fig. 3). The success of TTSP for the blends demonstrated that thermorheological simplicity occurred through the β-transition, whereas a complex behavior was observed in the vicinity of the α-transition. Similar thermorheological behavior has been observed for other semicrystalline polymers.[29] Hence, the fragility analysis was conducted around the β-transition. For pure PP and the binary blends, an Arrhenius trend is observed in the fragility plots (Fig. 4). Slightly higher activation energy results from the addition of 2 and 5% MAPP but are likely not significant in light of the measurement error and similar results obtained in Figure 4 (Table III). Further, values within the range of error for m are observed for PP and all blends with MAPP addition. In other words, the addition of MAPP to the PP matrix does not appear to greatly modify the intermolecular cooperativity around the β-relaxation of PP. Also, note that the m value obtained in this study tends to be higher than those obtained by others with $m = 137$ for atactic PP.[30] However, Ngai and Roland have found that although the shape of the

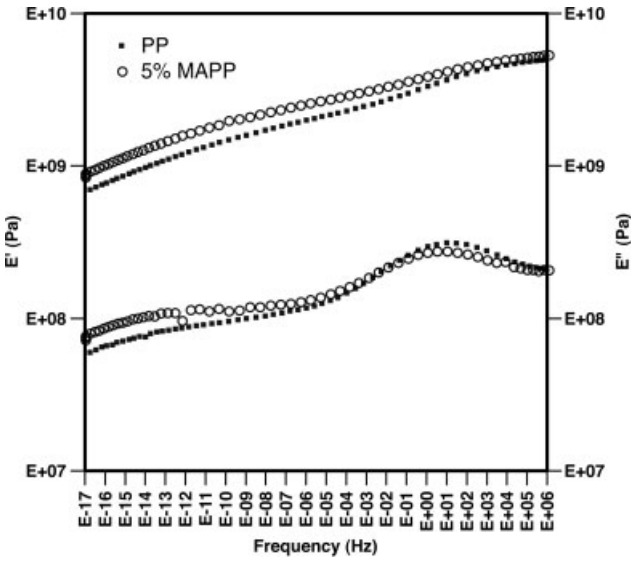

Figure 3 Typical Master curve obtained by TTSP on for 100% PP and 95% PP/5% MAPP blend.

relaxation is different in atactic PP as opposed to PP, their normalized temperature dependence is equivalent by having similar m values.[28] Ngai and Roland's observation suggests that the fragility for the blends studied in this work is dependent only on the molecular interactions in the amorphous fraction of the PP and not the polar groups in the copolymer. Thus, the low addition levels of MAPP in this study assert very little influence on scaling about T_g.

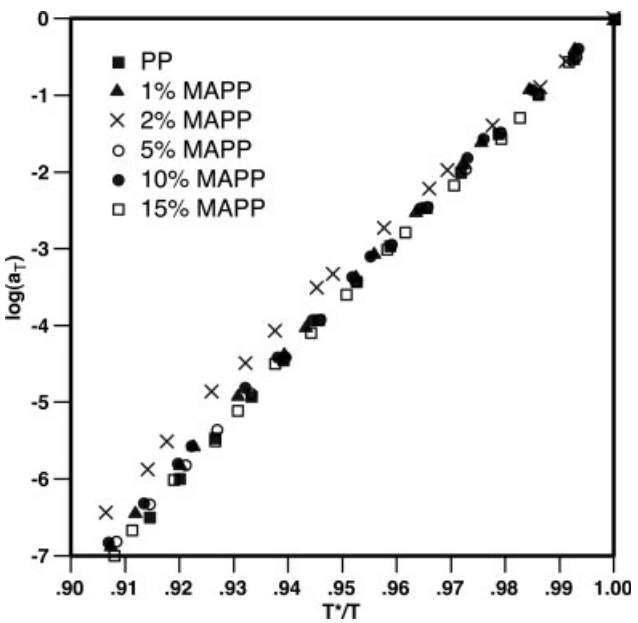

Figure 4 Cooperativity plots comparing neat PP to blends with MAPP. The reference temperature, T^*, corresponds to the maximum in E'' from the 1 Hz frequency scans at 2° steps.

TABLE III
The Activation Energies for the β Relaxation ($E_{a,\beta}$) Calculated from the Shift Factors and the Fragilities (m)

Blend	$E_{a,\beta}$ (kJ/mol) (±7 kJ/mol)[a]	m (±4)[a]
PP	371	175
1% MAPP	371	168
2% MAPP	386	175
5% MAPP	394	179
10% MAPP	373	170
15% MAPP	371	168

The fragility was normalized with respect to T^*.
[a] The error was estimated to be the largest standard error obtained from the regression analysis.

CONCLUSIONS

DSC analysis of PP/MAPP blends indicated that MAPP might cocrystallize with PP as observed by increasing melt point depression with increasing MAPP content. The miscibility of the polymers does not impart any change on the location of the β-transition as observed in some systems. This suggests that the miscibility of MAPP and PP is more important in the crystalline phase than in the amorphous phase. The addition of small amount of MAPP leads to a slight increase in E' in the glassy state for the blend over PP. This increase over PP is negligible past the β-transition. The consequence is little to no increase in stiffness in rubbery state, but a decrease in damping ability around the β-transition compared with PP alone. Most importantly, the addition of small amounts of a polar copolymer does not seem to influence the molecular coupling between PP chains. The only notable change was a decrease in the melt stability of PP crystallites by introducing possible defects. Consequently, incorporation of small amounts MAPP into PP melts is expected to have little impact on the mechanical behavior of the blend over neat PP.

The authors acknowledge Honeywell Corporation for providing the copolymer.

References

1. Harper, D. P. Civil and Environmental Engineering; Washington State University: Pullman, WA, 2003.
2. Harper, D. P.; Wolcott, M. P. J Compos A 2004, 35, 385.
3. Bratawidjaja, A. S.; Gitopadmoyo, I.; Watanabe, Y.; Hatakeyama, T. J Appl Polym Sci 1989, 37, 1141.
4. Roland, C. M.; Ngai, K. L. Macromolecules 1992, 25, 363.
5. Bohmer, R.; Ngai, K. L.; Angell, C. A.; Plazek, D. J. J Chem Phys 1993, 99, 4201.
6. Ngai, K. L.; Plazek, D. J. Macromolecules 1990, 23, 4282.
7. Jin, X.; Zhang, S. H.; Runt, J. Macromolecules 2003, 36, 8033.
8. Zhang, S. H.; Painter, P. C.; Runt, J. Macromolecules 2002, 35, 9403.
9. Scott, R. L. J Chem Phys 1949, 17, 279.
10. Lo, C. T.; Seifert, S.; Thiyagarajan, P.; Narasimhan, B. Polymer 2004, 45, 3671.
11. Keith, H. D.; Padden, F. J. J Appl Phys 1964, 35, 1270.
12. Avrami, M. J Chem Phys 1939, 7, 1103.
13. Hoffman, J. D.; Davis, G. T.; Lauritzen, J. I. Treatise on Solid State Chemistry; Plenum Press: New York, 1976.
14. Clark, E. J.; Hoffman, J. D. Macromolecules 1984, 17, 878.
15. Hoffman, J. D.; Weeks, J. J. J Chem Phys 1963, 37, 1723.
16. Marand, H.; Xu, J.; Srinivas, S. Macromolecules 1998, 31, 8219.
17. Wolcott, M. P.; Chowdhury, M.; Harper, D. P.; Li, T.; Heath, R.; Rials, T. G. The 6th International Conference on Wood-fiber-Plastic Composites, Madison, WI, 2001.
18. Liu, T.; Petermann, J. Polymer 2001, 42, 6453.
19. Liu, T.; Petermann, J.; He, C.; Liu, Z.; Chung, T. S. Macromolecules 2001, 34, 4305.
20. Schmidtke, J.; Strobl, G.; ThurnAlbrecht, T. Macromolecules 1997, 30, 5804.
21. Supaphol, P.; Spruiell, J. E. J Appl Polym Sci 2000, 75, 44.
22. Zhou, W.; Cheng, S. Z. D.; Putthanarat, S.; Eby, R. K.; Reneker, D. H.; Lotz, B.; Magonov, S.; Hsieh, E. T.; Geerts, R. G.; Palackal, S. J.; Hawley, G. R.; Welch, R. B. Macromolecules 2000, 33, 6861.
23. Wunderlich, B. In Thermal Characterization of Polymeric Materials; Turi, E., Ed.; Academic Press: Philadelphia, Pennsylvania, 1981; pp 91–234.
24. Harper, D. P.; Wolcott, M. P. Appl Spectrosc 2006, 60, 898.
25. Duvall, J.; Sellitti, C.; Myers, C.; Hiltner, A.; Baer, E. J Appl Polym Sci 1994, 52, 207.
26. Boyd, R. H. Polymer 1985, 26, 323.
27. Behzad, M.; Tajvidi, M.; Ehrahimi, G.; Falk, R. H. Int J Eng Transact B: Appl 2004, 17, 95.
28. Ngai, K. L.; Roland, C. M. Macromolecules 1993, 26, 2688.
29. Wortmann, F. J.; Schulz, K. V. Polymer 1995, 36, 1611.
30. Plazek, D. J.; Ngai, K. L. Macromolecules 1991, 24, 1222.